Indian Journal of Biochemistry & Biophysics
Vol. 61, February 2024, pp. 105-117
DOI: 10.56042/ijbb.v61i2.6922

Preparation and evaluation of spray dried powder of *Trigonella foenum-graecum* seeds as suspending agents to develop rivaroxaban nanosuspension

Rama Rao Nadendla[1]*, KRS Sambasiva Rao[2], Sandeep Kanna[1], Juluri Satyanarayana[1] & Charugulla Mrudhvani[1]

[1]Chalapathi Institute of Pharmaceutical Sciences, Chalapathi Nagar, Guntur-522 034, Andhra Pradesh, India

[2]Department of Pharmacy, Mangalayatan University-Jabalpur, Jabalpur-483 001, Madhya Pradesh, India

Received 24 November 2023; *revised 24 January 2024*

The present study aimed to formulate rivaroxaban nanosuspension by nanoprecipitation with the ultrasonication method and was stabilized by different concentrations of Fenugreek Seed Mucilage, Microcrystalline Cellulose and Carboxymethyl Cellulose. The formulated nanosuspensions were evaluated for saturation solubility studies, particle size, drug content, zeta potential, and *in vitro* drug release. In the FT-IR spectra of the drug in the physical mixture, it was noted that the peaks had remained unaltered. DSC thermograms of Rivaroxaban and the physical mixture indicated the absence of interaction and the presence of the drug in an unchanged form. The evaluation tests were conducted and optimization was done using Minitab software. Optimized formulation F3 demonstrated an impressive saturation solubility of 0.89 mg/mL. The particle size distribution studies revealed that the optimized formulation F3 showed 79 nm. Formulation F3 exhibited drug content reaching 75%. The zeta potential was measured at -33 mV for formulation F3. Pure drug RN exhibited a cumulative drug release of 20%, and formulation F3 showed 71% cumulative drug release at the end of the 60th min. Rivaroxaban nanosuspension showed a prolonged duration of drug action, enhanced the rate and extent of drug absorption, and ultimately increased the therapy's effectiveness.

Keywords: Minitab, Mucilage, Rivaroxaban, Zeta potential

Nanotechnology has emerged as a notable accomplishment of 21st century science. This interdisciplinary field encompasses the synthesis, manipulation, and utilization of materials measuring less than 100 nanometres in size. Nanoparticles find valuable applications across various sectors, including environmental management, agriculture, food production, biotechnology, biomedicine, and pharmaceuticals. For instance, they play pivotal roles in treating[1], monitoring environmental conditions[2], serving as functional food additives[3], and acting as potent antimicrobial agents[4].

Nanotechnology presents numerous benefits when contrasted with traditional technologies. It can improve solubility, dissolution rates, extend oral bioavailability, and decrease the necessary dosage. Multiple drug delivery systems harness nanotechnology, encompassing nanosuspensions, solid lipid nanocrystals, and nanoemulsions. Among these, nanosuspension preparation distinguishes itself due to its technical simplicity and cost-effectiveness compared to alternative nanosizing techniques[5, 6].

Correspondence:
E-mail: nadendla2000@yahoo.co.in

A nanosuspension is a colloidal dispersion of drug particles within an aqueous medium, often water, stabilized by surfactants, polymers, or a blend of both[7]. It can be produced through three principal approaches: bottom-up technology, top-down technology, or a fusion of both. Bottom-up technology encompasses precipitation techniques. Conversely, top-down methods involve media milling, high-pressure homogenization in aqueous and non-aqueous media, and a combination of precipitation and high-pressure homogenization[8,9].

Rivaroxaban (RN), an oral anticoagulant derived from the oxazolidinone class, prevents venous thromboembolism in adult patients undergoing full hip or knee replacement surgery. This medication serves as a potent and selective direct inhibitor of factor Xa[10]. Rivaroxaban is characterized by its small molecular size, with a molecular mass of 436 g mol^{-1}, and it exhibits substantial plasma protein binding in humans, ranging from 92% to 95%. The primary binding partner in serum albumin[11,12].

Fenugreek (*Trigonella foenum-graecum*; Fabaceae) is a plant whose seeds and leaves hold significance in traditional medicine. The utilization of fenugreek

primarily hinges on the abundance of flavonoids and polyphenols it contains. This plant has been documented to exhibit anti-inflammatory properties, primarily attributed to its flavonoid content[13,14]. Flavonoids serve as antioxidants and potential inhibitors of enzymes like cyclooxygenase, lipoxygenase, and nitric oxide synthase. Moreover, fenugreek finds extensive application for various purposes within the field of pharmaceutical sciences[15].

Microcrystalline cellulose (MCC) is a purified and partially depolymerised form of cellulose with the chemical formula $(C6H10O5)_n$. It is created by treating alpha cellulose with mineral acids of type Ib. This polysaccharide polymer comprises a linear chain of several hundred to tens of thousands of β(1→4) linked D-glucose units, forming linear chains of β-1,4-D anhydro glucopyranosyl units. The raw material employed for MCC production typically originates from fibrous plants, such as conifer wood. Cotton also serves as a potential cellulose source for MCC[16,17]. In the case of pharmaceutical-grade MCC, which requires high-quality pulp, wood remains the most common source.

CMC (Carboxymethyl cellulose) is a cellulose derivative characterized by carboxymethyl groups. These groups are introduced through a reaction between cellulose and chloroacetate in an alkaline environment, leading to substitutions in the glucose units' C2, C3, or C6 positions within cellulose[18]. Consequently, CMC becomes water-soluble and more susceptible to the hydrolytic action of cellulases. Due to its water-soluble nature and increased susceptibility to enzymatic hydrolysis, CMC serves as a valuable additive in both liquid and solid media for detecting cellulase activity and measuring cellulose hydrolysis[19].

This study aimed to formulate a nanosuspension of Rivaroxaban (RN) through a precipitation ultrasonication technique and to prolong the duration of drug action, enhance the rate and extent of drug absorption, and ultimately increase the effectiveness of therapy.

Materials and Methods

Rivaroxaban was received as a gift sample from Alphamed formulations, Hyderabad. Spray dried mucilage of "*Trigonella foenum-graecum*" and Liquid sugar was obtained at Chalapathi Institute of Pharmaceutical Sciences, Lam. Carboxymethyl cellulose and microcrystalline cellulose were purchased from Signet Pvt. Ltd, Mumbai. Sodium saccharin and Methyl paraben were also obtained as a gift sample from Alphamed formulations, Hyderabad. TWEEN 80 was purchased from Loba chemie. Glycerol and acetone were purchased from Thermo Fisher Scientific Pvt. Ltd., Mumbai.

Methods

Preformulation studies

Excipients assumed a crucial role in enhancing the stability, dissolution, and compatibility of rivaroxaban in the selected dosage forms. Various polymers, including microcrystalline cellulose (MCC), and Carboxymethyl cellulose (CMC), were scrutinized for their capacity to stabilize the drug and influence its release profile. The addition of the spray-dried powder of *Trigonella foenum-graecum* and Tween 80 as a surfactant aimed to improve the wetting and dissolution of the drug. Compatibility studies, employing techniques such as Differential Scanning Calorimetry (DSC) and Fourier Transform Infrared Spectroscopy (FTIR), were executed to verify the compatibility between the drug and the chosen excipients[20].

FTIR Spectroscopy

FT-IR spectra were obtained for RN (Rivaroxaban), as well as for physical mixtures of RN with selected pharmaceutical excipients, including fenugreek seed powder, carboxymethyl cellulose microcrystalline cellulose, saccharin sodium, and methylparaben. The ratios of these mixtures were maintained at 1:1 weight/weight. The spectra were recorded using a BRUKER alpha model infrared spectrophotometer equipped with OPUS software. To create the samples, they were combined with IR-grade KBr at a ratio of 1:100 and then compressed into pellets using a pellet press. These resultant pellets were then subjected to scanning using an FT-IR spectrophotometer (BRUKER, alpha model) across the spectral range of 4000 cm^{-1} to 500 cm^{-1}. To ensure the absence of any changes in the principle peaks of the RN and excipients spectra, the FT-IR spectra of the physical mixtures were compared with the individual FT-IR spectra of RN and the excipients[21].

DSC (Differential scanning calorimetry)

DSC thermograms were acquired using the TA Q20 model from TA Instruments, operated with TAQ20 software. Thermal analysis was conducted for RN (Rivaroxaban), and RN combined with a physical

mixture of selected pharmaceutical excipients such as fenugreek seed powder, carboxymethyl cellulose, microcrystalline cellulose etc. The mixtures were prepared in a 1:1 weight/weight ratio. Homogeneous physical mixtures were directly weighed to approximately 2 mg within pierced DSC aluminium pans. The sample was subjected to equilibration and heating from 30°C to 400°C at a rate of 10°C/min under a dry nitrogen atmosphere. In this context, "zero air" prevented combustion, preserving heat and temperature stability. As the temperature reached 300°C, the curve was obtained, and the sample chamber was cooled by nitrogen gas[22].

Preparation of *Trigonella foenum-graecum* seed extract

Trigonella foenum-graecum seeds were sourced from the local market and thoroughly cleaned to eliminate impurities. The seeds were finely ground into a powder using an appropriate pulveriser. An accurate weight of approximately 12.5g of the powder was measured and then dispersed in 500 mL of water. The mixture was heated in a water bath at 70°C, while continuously stirred with a glass rod to prevent the formation of lumps. After 15 min, the color of the water changed to a pale yellow hue. The heat source was turned off, and the mixture was filtered through muslin cloth. The resulting filtrate was retained for subsequent spray drying. The spray dryer was set to operate at a temperature of 120°C, and the flow rate of the filtrate was adjusted to 23 rpm. After the spray drying process, the resulting powdered mucilage was collected and weighed[23].

Preparation of nanosuspensions

Rivaroxaban (RN) nanosuspensions were prepared through the precipitation ultrasonication method. In this study, three distinct nanosuspension formulations were created, employing diverse stabilizers, including mucilage from "*Trigonella foenum-graecum*" seed as a natural polymer, carboxymethyl cellulose, and microcrystalline cellulose, each in varying proportions as detailed in the (Table 1).

The initial step involved dissolving the stabilizers in the aqueous phase and adding components like surfactant TWEEN 80, sweetening agents like liquid sugar and sodium saccharin, and preservatives like methylparaben. Separately, 200 mg of the rivaroxaban drug was dissolved in acetone, serving as the organic phase. Subsequently, the organic phase was cautiously introduced drop by drop into the aqueous phase while being subjected to ultra turrax homogenization at 8000 rpm for 5 min, which aimed to pre-mill the coarse suspensions. This step facilitated the gradual evaporation of the organic solvent from the coarse suspension. The resulting suspension underwent ultrasonication to reduce its particle size, yielding a nanosuspension. The ultrasonication process utilized the Oscar ultraprobe sonicator PR-250Mp for 30 min, with a pulse time of 5 min.

Finally, the prepared nanosuspensions were transferred into amber-colored containers for storage, and a comprehensive evaluation of various parameters was conducted to obtain the results[24].

Evaluation of RN nanosuspensions

Saturation solubility studies

Excess amounts of drug RN, along with physical mixtures and RN nanosuspensions that had been formulated, were introduced into separate 10 mL portions of phosphate buffer (pH 6.8). These samples were then placed in a water bath maintained at 25°C with continuous rotation at 20 rpm for 48 h. Following this incubation period, the samples were filtered, suitably diluted, and subsequently analyzed spectrophotometrically at a wavelength of 244 nm[25].

Table 1 — Nanosuspension formulations

Ingredients	F1	F2	F3	F4	F5	F6	F7	F8	F9	F10	F11	F12	F13
Rivaroxaban (mg)	200	200	200	200	200	200	200	200	200	200	200	200	200
Trigonella foenum-graecum seed mucilage (mg)	0	20	40	0	40	20	0	40	20	40	40	0	0
Carboxymethyl cellulose (mg)	600	0	0	0	0	300	0	600	600	300	600	600	300
Microcrystalline cellulose (mg)	0	0	600	300	0	300	600	0	600	600	300	600	0
Sodium saccharin (mg)	0.5	0.5	0.5	0.5	0.5	0.5	0.5	0.5	0.5	0.5	0.5	0.5	0.5
Liquid sugar (mL)	7	7	7	7	7	7	7	7	7	7	7	7	7
Methyl paraben (%)	0.2	0.2	0.2	0.2	0.2	0.2	0.2	0.2	0.2	0.2	0.2	0.2	0.2
Tween 80 (mL)	1	1	1	1	1	1	1	1	1	1	1	1	1
Glycerol (mL)	1	1	1	1	1	1	1	1	1	1	1	1	1
Water (mL)	200	200	200	200	200	200	200	200	200	200	200	200	200

Determination of particle size and polydispersity index

Particle size analysis for all formulations was conducted using the Horiba Scientific Nanoparticle Size Analyzer (SZ-100-Z). To prepare the samples, a small quantity of dry RN nanoparticles was diluted in double-distilled water at twice the nanoparticle amount. This mixture was continuously stirred for 1 h and then filtered through a 0.45 µM Millipore filter to obtain the desired nanoparticle dispersion. The mean particle size of the nanosuspensions was subsequently determined. The polydispersity index (PDI) was also evaluated using the Horiba Scientific Nanoparticle Size Analyzer (SZ-100-Z). PDI serves as an indicator of the variation within the particle size distribution. Monodisperse samples display lower PDI values, whereas higher PDI values indicate a broader particle size distribution, suggesting a polydisperse nature of the samples[26]. PDI can be calculated using the following equation:

Polydispersity = [D90 – D10] / D50

Drug content

A quantity of drug-loaded RN nanosuspension equivalent to 1 mg was initially dissolved in fifty millilitres of a mixture consisting of ACN/water (50:50 *v/v*). This resulting mixture was then sonicated for 15 min to ensure complete drug extraction. Subsequently, the flask was adjusted to its final volume. An aliquot of the solution was filtered through a 0.45 µM membrane filter. The resulting final solutions were diluted with ACN/water (50:50 *v/v*) to a final volume of 10 mL, using buffer at pH 6.8. The mixture was stirred continuously for 2 h. The final suspension underwent ultra-centrifugation at 10,000 rpm for 30 min. The supernatant was carefully collected, appropriate dilutions were carried out, and the quantity of RN was determined through spectrophotometric measurements at a wavelength of 248 nm[27].

Determination of zeta potential

The Horiba Scientific Nanoparticle Size Analyzer (SZ-100-Z) determined the zeta potential of appropriately diluted nanosuspensions. This analysis provided information about the charge on nanoparticles, their mean zeta-potential value, and the standard deviation (SD) based on three measurements[28].

Scanning electron microscopy (SEM)

Particle morphology was assessed using a scanning electron microscope (SEM), specifically the JSM 6360 model by JEOL Japan. A small droplet of the suspension was initially air-dried and oven-dried to prepare the samples for observation. The resulting dried sample was then attached to double-sided adhesive tapes and subjected to gold coating (20 mA) under reduced pressure (0.001) for 5 min using an ion sputtering device. After the gold-coating procedure, the samples were examined using the SEM. Photomicrographs at appropriate magnifications were captured to visualize the particle morphology[29].

***In vitro* drug release**

The *in-vitro* release profiles of pure RN and the various formulations (F1-F13) were assessed utilizing the dialysis diffusion technique. An accurately measured quantity of pure RN (5 mg) and nanosuspensions equivalent to 5 mg of the drug were transferred into a dialysis bag with a molecular weight cut off of 12000 – 14000 Da, and then securely sealed. This sealed bag was suspended within a USP Type II apparatus containing 900 mL of phosphate buffer at pH 6.8. The apparatus operated at a constant speed of 50 rpm, maintaining a bath temperature of 37°C ± 0.5°C. At predetermined intervals, 5 mL aliquots of the sample were withdrawn from the receptor compartment, and the same volume was replaced with fresh buffer to maintain sink conditions. Drug release was quantified spectrophotometrically after appropriate dilution, measuring the absorbance at 244 nm, with the phosphate buffer at pH 6.8 serving as the blank[30].

Results

Compatibility studies

FT-IR Spectroscopy

The interaction between the drug and the carrier often leads to noticeable changes in physical mixtures' infrared (IR) profile. The FTIR spectra of the pure drug (Fig. 1) revealed distinct absorption bands at specific wave numbers 3355 cm^{-1}, attributed to secondary amide (N-H) stretching. 1736 cm^{-1}, corresponding to C-O stretching originating from the ester group. Bands in the range of 1670-1640 cm^{-1}, representing amide stretching. Bands between 1575-1500 cm^{-1}, indicating Ar-Cl stretching and N-H scissoring. Bands within the 1340-1000 cm^{-1} range correspond to C-O-C movements found in both esters and ethers. Peaks at 850-550 cm^{-1}, corresponding to C-Cl stretching. Upon analyzing the FTIR spectra of the drug in the physical mixture (Fig. 2), it was noted that the peaks had remained unaltered, retaining their distinctive characteristics. This absence of changes in

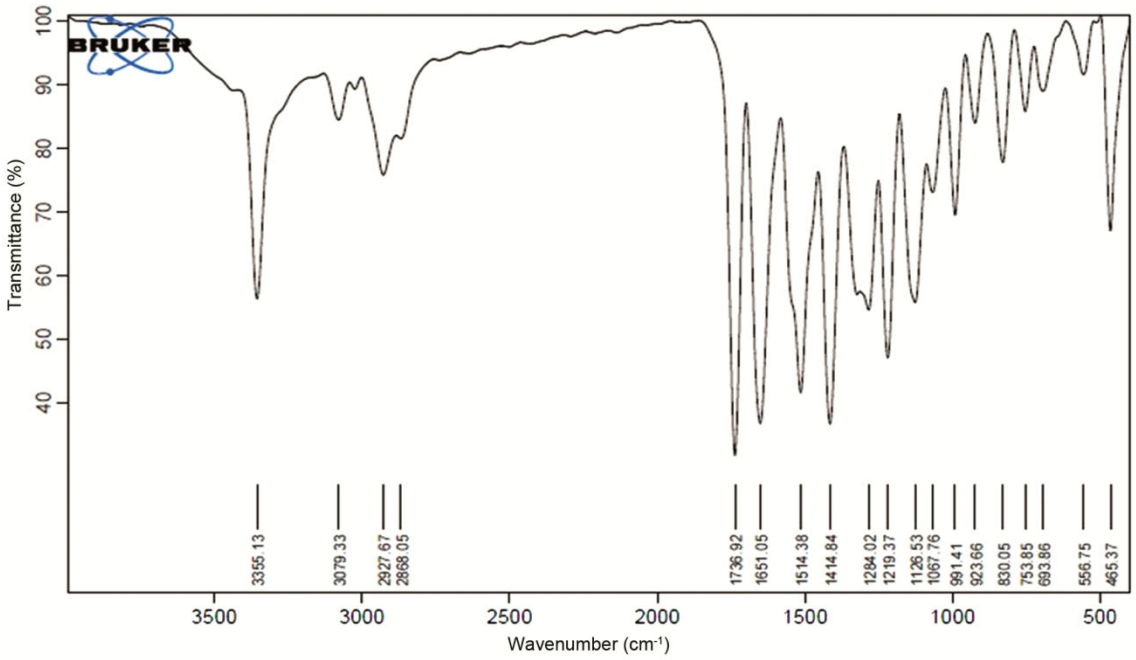

Fig 1 — FT-IR Spectrum of Pure Drug

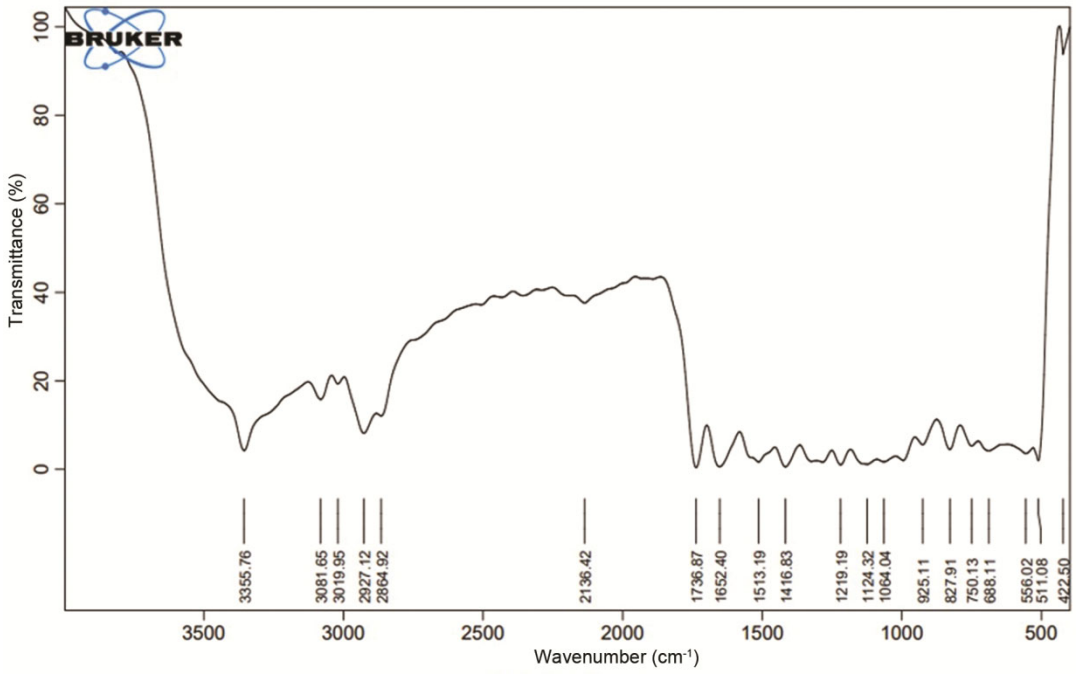

Fig. 2 — FT-IR Spectrum of Physical Mixture

peak characteristics implies no discernible interaction between the drug and the excipients.

DSC studies

Differential Scanning Calorimetry (DSC) facilitated quantitative identification of energy consumption or release processes, such as endothermic and exothermic phase transformations. In the DSC curve, a solitary endothermic peak associated with the melting point was identified at 229.27 °C for pure drug (in fig. 3) and a comparable endothermic peak was observed at 231.40 °C for the physical mixture (in fig. 4). The comparison of endothermic peaks from both the DSC curve of

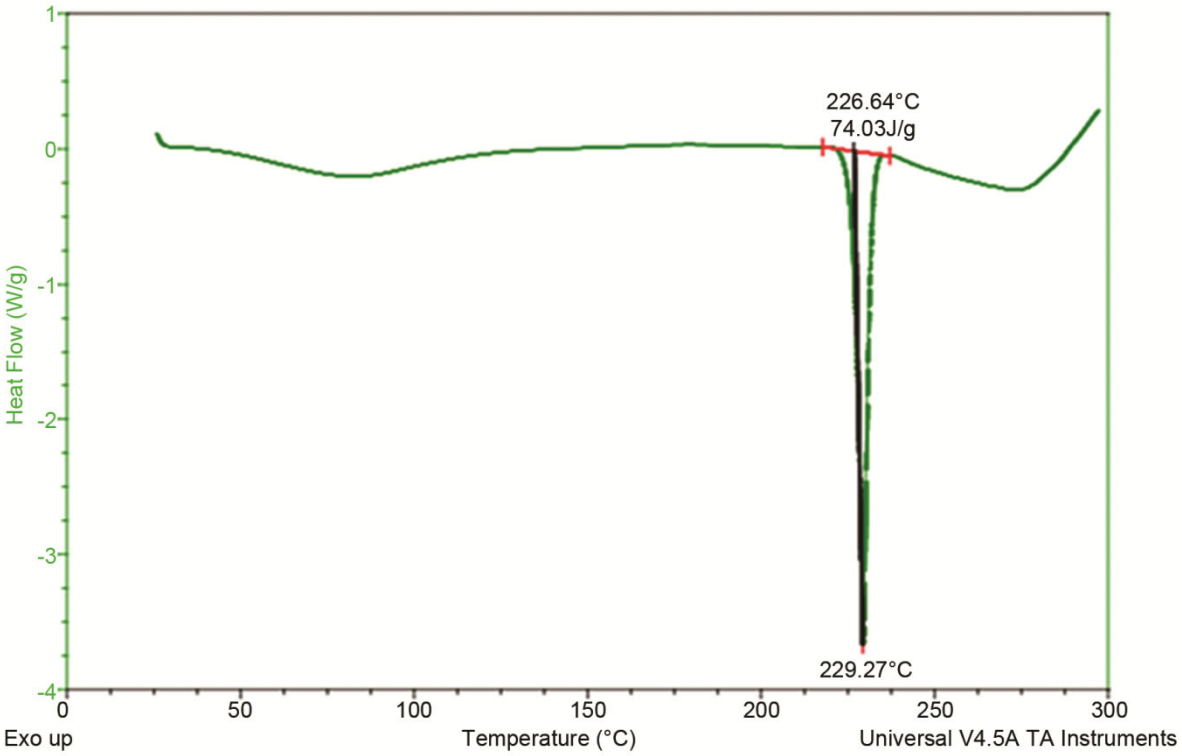

Fig. 3 — Thermogram of Pure Drug

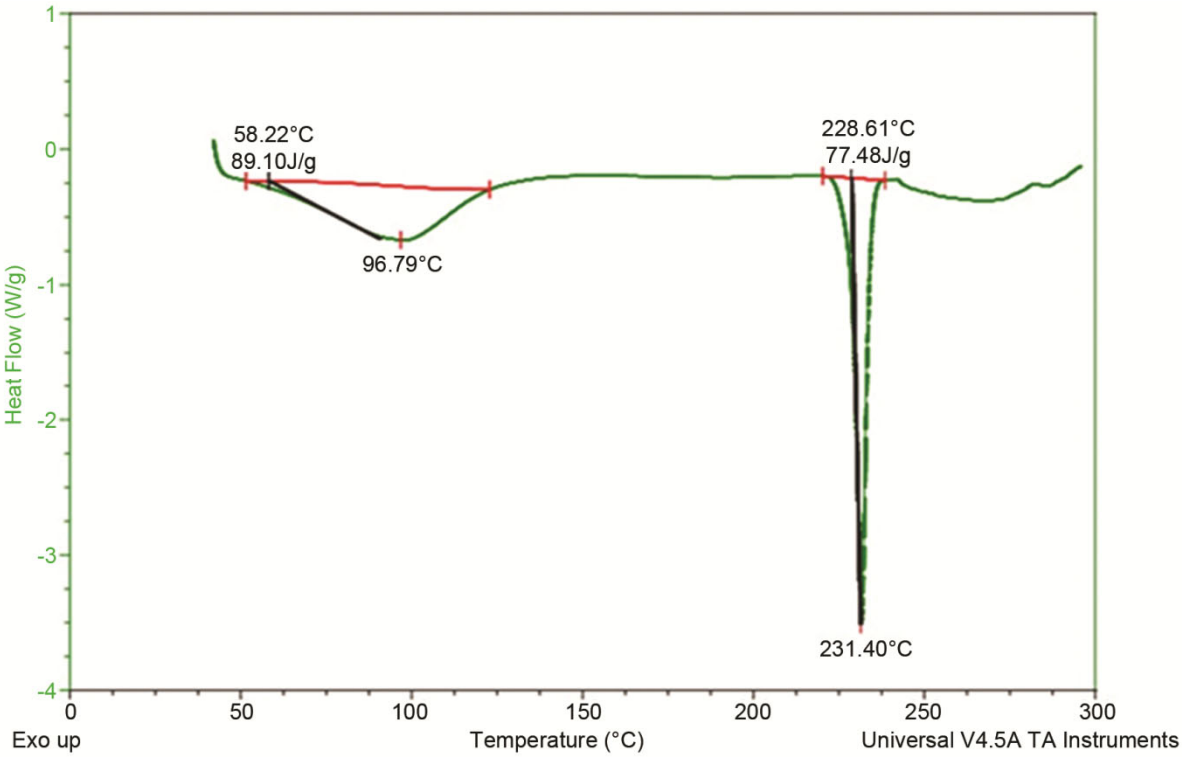

Fig. 4 — Thermogram of Physical Mixture

Rivaroxaban and the physical mixture indicated the absence of interaction and the presence of the drug in an unchanged form.

Preparation of nanosuspension

The investigation aimed to develop RN nanosuspensions using ultrasonic precipitation, with formulations incorporating spray-dried powder of *Trigonella foenum-graecum*, MCC & CMC. Through the ultrasonic precipitation method, all RN nanosuspensions (F1 – F13) were successfully formulated and are subjected to evaluation for factors such as particle size, stability, and overall effectiveness. *Trigonella foenum-graecum*, MCC and CMC serve as key components in these formulations.

Experimental design

The nanosuspension formulations that were prepared underwent essential evaluation tests. These nanosuspensions were examined for particle size, zeta potential, and *in vitro* drug release studies (Table 2). The evaluation tests were conducted and optimization was done using Minitab software.

Screening design model: Particle Size versus Mucilage, MCC, CMC

The formulations exhibited a particle size range between 78 to 300 nm. The equation derived from the most suitable mathematical model to represent the response R1 (particle size in relation to mucilage, MCC, CMC) was R1 = 224.3 - 3.480 Mucilage + 0.0373 MCC - 0.0493 CMC. In this scenario, mucilage, MCC, and CMC were significant terms in the model, with Prob > F values less than 0.00500. The predicted R^2 value aligned well with the adjusted R^2 value. The analysis of particle size data revealed negative coefficients for mucilage and CMC, while a positive coefficient was observed for MCC. A positive coefficient signifies a synergistic effect, while a negative coefficient suggests an antagonistic effect. The residuals in the normal probability plot followed a normal distribution and formed a linear pattern. The plots of residuals versus predicted and residuals versus run showed no patterns in the error terms, confirming the model's suitability for the obtained data from the software. The 3D response surface plot demonstrated a significant reduction in particle size with increased concentrations of mucilage and CMC variables (Figs 5 & 6).

Screening design model: Zeta Potential versus Mucilage, MCC, CMC

The formulations exhibited zeta potential values ranging from -8 to -33 mVs. The equation derived from the most suitable mathematical model to represent the response R2 (zeta potential in relation to mucilage, MCC, CMC) was R2 = -12.54 - 0.3100 Mucilage + 0.00267 MCC - 0.00867 CMC. In this context, mucilage, MCC, and CMC were significant terms in the model, with Prob > F values less than 0.00500. The predicted R^2 value closely matched the adjusted R^2 value. The residuals in the normal probability plot exhibited a normal distribution and formed a linear pattern. The plots of residuals versus predicted and residuals versus run showed no discernible patterns in the error terms, indicating that the model was well-suited to the data obtained from the software. The 3D response surface plot illustrated a substantial decrease in zeta potential with increasing concentrations of mucilage and CMC variables (Figs 7 & 8).

Screening design model: % Drug Release versus Mucilage, MCC, CMC

The formulations, designated as F1 to F13, displayed drug release within the range of 80% to 92%. The equation derived from the most suitable

Table 2 — DoE chart for nanosuspension formulations

S. No.	Formulations	Mucilage	MCC	CMC	Particle Size	Zeta Potential	% Drug Release
1	F1	0	600	0	250	-10	80
2	F2	20	0	0	120	-20	85
3	F3	40	0	600	78	-33	90
4	F4	0	0	300	180	-18	83
5	F5	40	0	0	98	-25	92
6	F6	20	300	300	100	-22	90
7	F7	0	0	600	200	-15	80
8	F8	40	600	0	98	-25	90
9	F9	20	600	600	100	-25	85
10	F10	40	300	600	100	-23	88
11	F11	40	600	300	100	-25	85
12	F12	0	600	600	240	-18	80
13	F13	0	300	0	300	-8	80

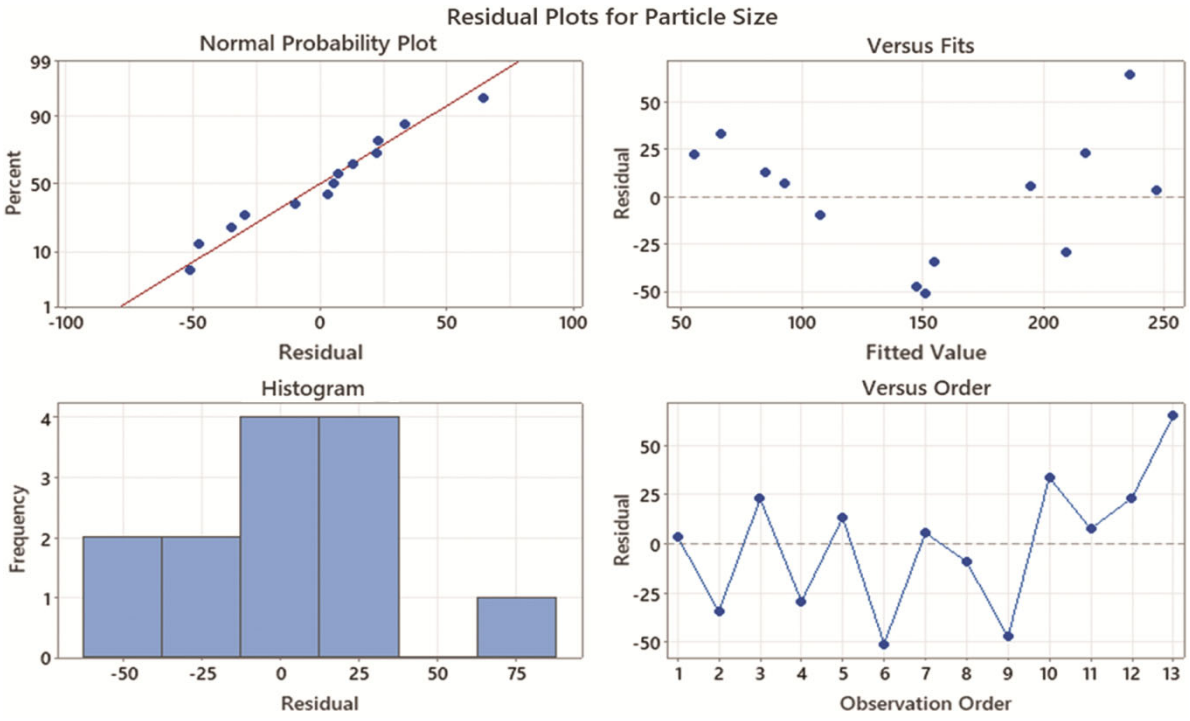

Fig. 5 — Residual plots for Response R1

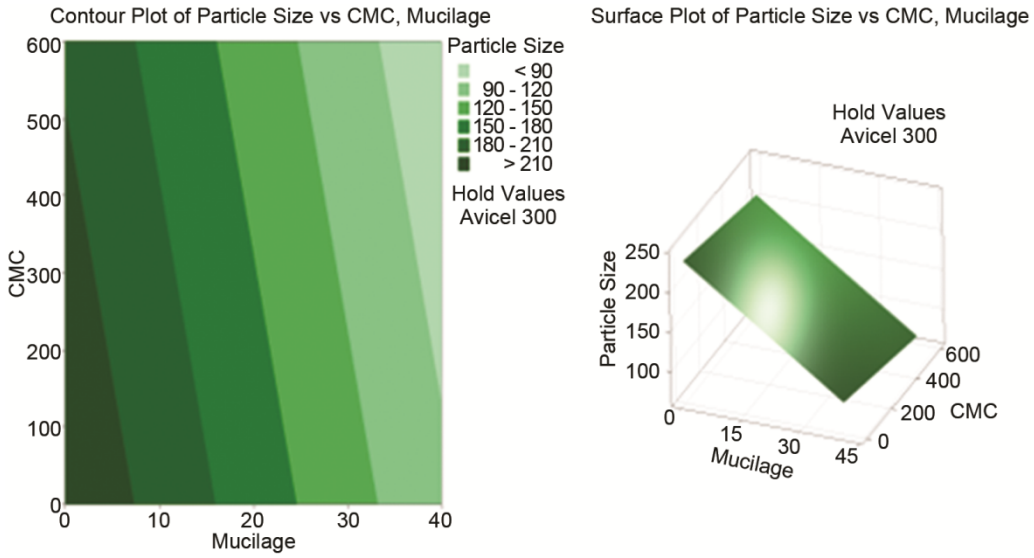

Fig. 6 — Contour plot and 3D response surface graph for Response R1

mathematical model to depict the response R3 (drug release in relation to mucilage, MCC, CMC) was R3 = 82.43 + 0.2100 Mucilage - 0.00333 MCC - 0.00133 CMC. In this context, mucilage, MCC and CMC were significant terms in the model, with Prob > F values less than 0.00500. The predicted R^2 value is closely aligned with the adjusted R^2 value. The residuals in the normal probability plot followed a normal distribution and exhibited a linear pattern. The plots of residuals versus predicted and residuals versus run demonstrated no discernible patterns in the error terms, indicating that the model effectively captured the data obtained from the software. The 3D response surface plot, as depicted in the figure, displayed a notable decrease in the percentage of drug release with an increase in the concentration of MCC and CMC variables (Figs 9 & 10).

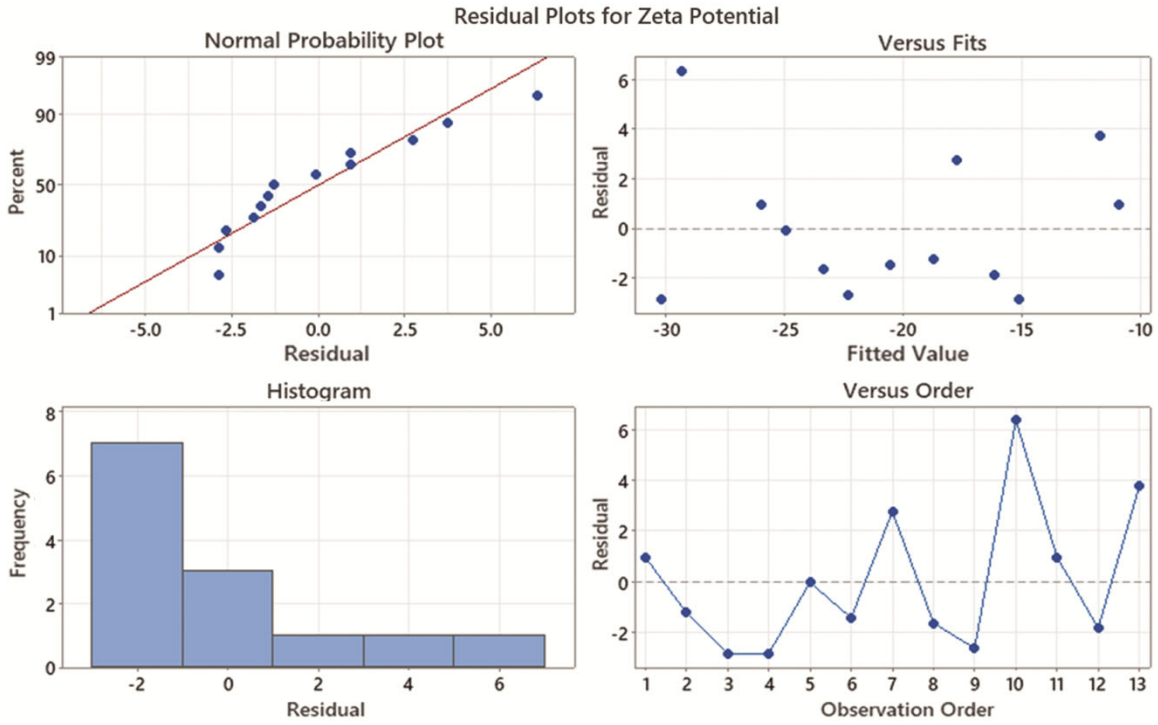

Fig. 7 — Residual plots for Response R2

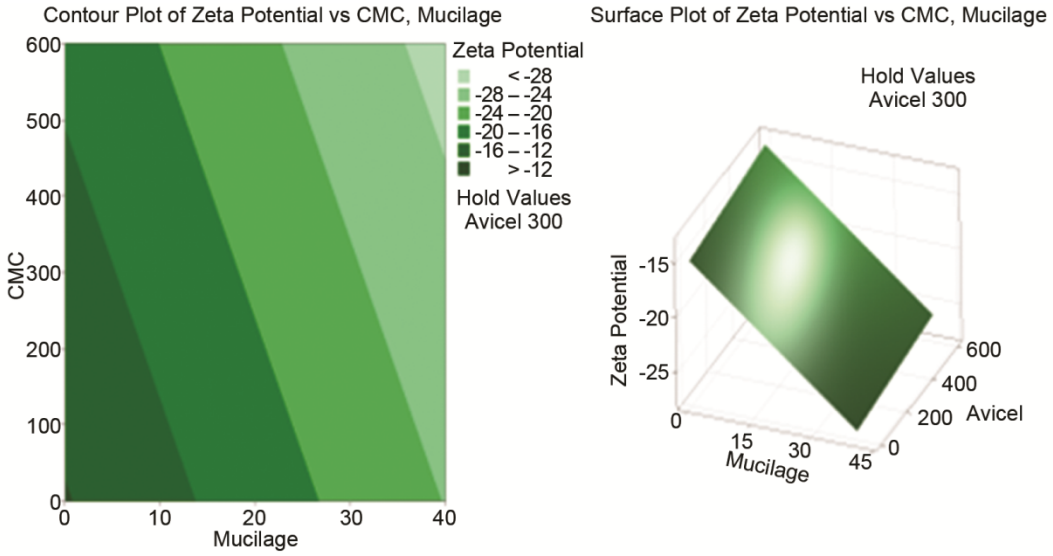

Fig. 8 — Contour plot and 3D response surface graph for Response R2

Evaluation of formulated nanosuspension

Saturation solubility studies

The pure drug RN demonstrated a saturation solubility of 0.09 mg/mL. Remarkably, the optimized formulation F3 exhibited saturation solubility of 0.89 mg/mL. This notable improvement can be credited to the incorporation of mucilage from "*Trigonella foenum-graecum*" seed, a hydrophilic polymer enhancing wettability, and Tween 80, a surfactant diminishing interfacial tension between phases. Noteworthy is the substantial augmentation in saturation solubility observed in the nanosuspension formulations. This significant enhancement is attributed to the reduction of drug particles to the nano-sized range, thereby increasing the effective surface area of these particles.

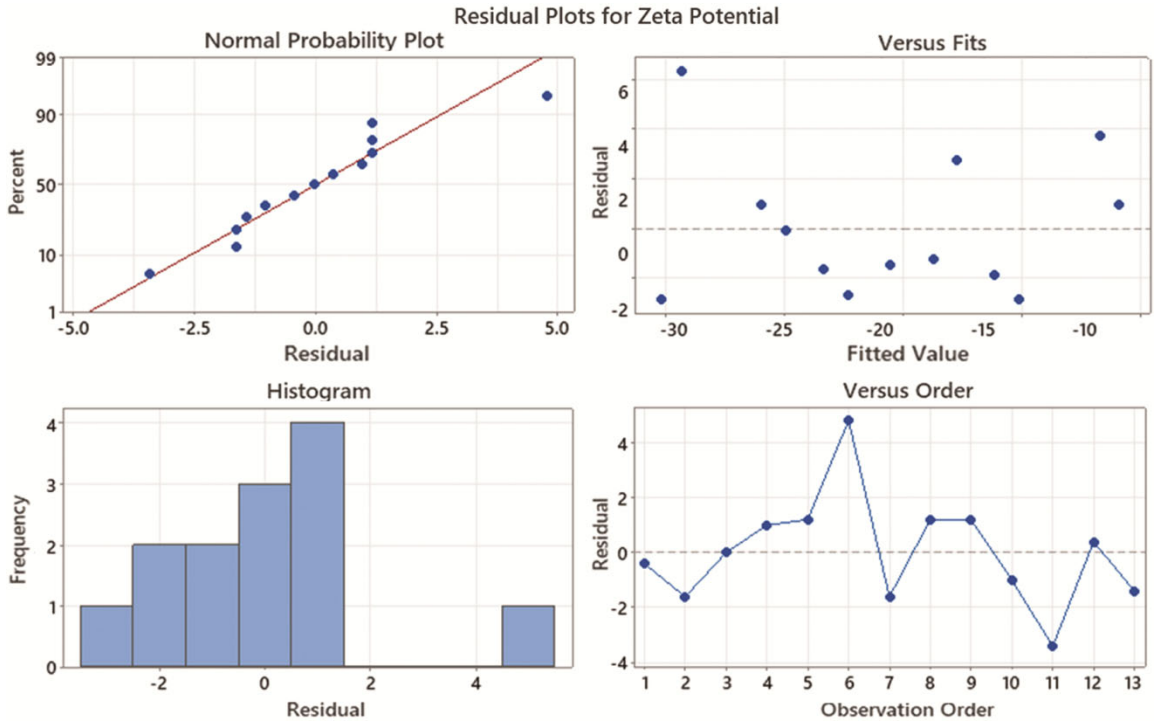

Fig. 9 — Residual plots for Response R1

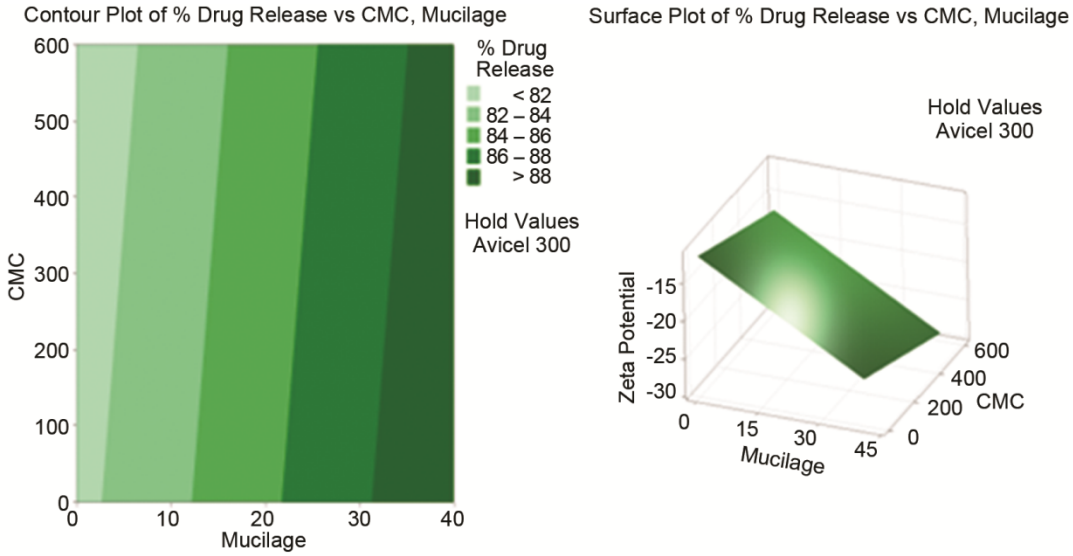

Fig. 10 — Contour plot and 3D response surface graph for Response R3

Particle size and polydispersity index

To confirm that the particles fell within the nano-range was crucial, necessitating particle size measurement. Particle size distribution studies for formulation F3 unveiled particles measuring 78 nm. The mean Polydispersity Index (PDI) values of the optimized formulation F3 displayed 0.231, indicating a commendable uniformity in particle size distribution.

Drug content

The drug content in the optimized formulation F3 was determined to be 75%. Notably, the concentration of mucilage from "*Trigonella foenum-graecum*" seed in the formulation exerted a significant impact on drug content. An increase in the concentration of mucilage led to an elevation in drug content. This phenomenon can be attributed to the heightened

viscosity of the solution, causing a delay in the diffusion of the drug from the layer, consequently resulting in increased entrapment.

Zeta potential

Zeta potential serves as a critical parameter for evaluating the long-term stability of nanoparticles. It characterizes the surface charge of the particles, offering insight into the level of repulsion between closely charged particles within the dispersion, thereby preventing particle aggregation. In the case of the optimized F3 formulation, the Zeta potential was measured at -33 mV. The negative zeta potential of the nanosuspension may be attributed to the anionic nature of the polymer. The attainment of high potential values is crucial to ensuring a high-energy barrier, favouring good stability.

Scanning electron microscopy

In Fig. 11, the SEM image of RN nanosuspensions F3 is presented, revealing drug particles that have precipitated in a spherical shape with an approximate size of 78 nm. These particles are distinct and exhibit uniformity in size, showcasing a consistent and homogeneous distribution.

***In vitro* drug release studies**

In the *in-vitro* dissolution studies comparing pure RN drug and the optimized formulation F3, a notable increase in drug release was observed in the nanosuspensions compared to the pure drug. Specifically, the results indicated that the pure drug RN exhibited a cumulative drug release of 20%. In contrast, Nanosuspension F3 achieved a remarkable 71% cumulative drug release, as depicted in Fig. 12. It's important to highlight that, in general, as particle size increases, the release rate tends to decrease. This phenomenon is attributed to smaller particles having a higher surface area relative to their volume. Consequently, most of the drug is concentrated near or on the particle surface, making it readily available for release.

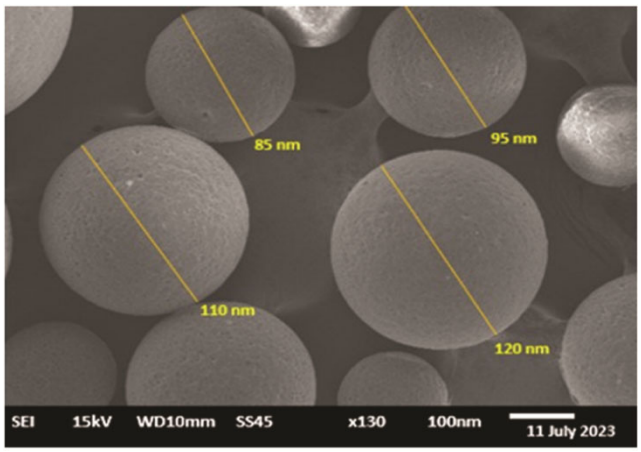

Fig. 11 — SEM image of Nanosuspension Formulation F3

Discussion

The research is aimed to develop a rivaroxaban nanosuspension through the precipitation ultrasonication method. Key components included Tween 80 as a surfactant, mucilage from "*Trigonella foenum-graecum*" seed as a natural polymer, and additional polymers such as carboxymethyl cellulose and Microcrystalline cellulose. Compatibility studies using FTIR and DSC confirmed the suitability of these components.

The optimization process, facilitated by Minitab software, identified formulation F3 as the optimal choice, exhibiting a particle size of 78 nm and a zeta potential of -33mV. The investigation into mucilage concentration revealed that higher concentrations increased particle size and drug content.

The stability assessment of the rivaroxaban nano suspension incorporating "*Trigonella foenum-graecum*" seed mucilage indicated favourable results, with particle sizes within the acceptable range and a good percentage yield.

In vitro studies demonstrated improved solubility and enhanced diffusion rates for the nanosuspension dosage form. The drug release pattern showed sustained release up to 60 min, with an initial fast release.

The precipitation ultrasonication method proved to be a convenient and efficient alternative to conventional methods. The rivaroxaban nano suspension, particularly formulation F3, exhibited

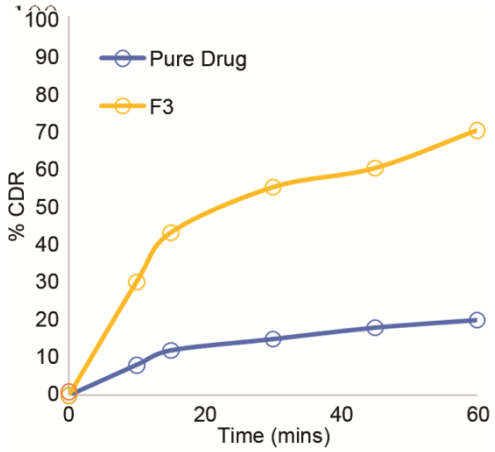

Fig. 12 — *In vitro* drug release graph

increased dissolution rates compared to the standalone drug, suggesting its potential as an orally active dosage form.

Conclusion

In the present study, Rivaroxaban nanosuspensions were successfully formulated by the emulsification solvent diffusion technique. The best nanosuspension formulation was found to be F3 with saturation solubility 0.89 mg/mL, particle size 78 nm, PDI 0.2, zeta potential -33mV, and Cumulative drug release of 71%. SEM images confirmed that the particle size of the formulation was in nano range. It can be concluded that formulated as nanosuspension formulation can enhance the dissolution and ultimately increased the therapy's effectiveness.

Conflict of interest

All authors declare no conflict of interest.

References

1 Singh M, Chauhan D, Gill R, Iqbal Z & Solanki P, Sustained release of drug loaded nanofibers for wound dressing applications. *Indian J Biochem Biophys,* 59 (2022) 479.

2 Dutta A, Dutta P, Kayal T, Ray S, Dutta M, Ghosh K, Biswas S, Sarkar S, Bera A, Saha M, Mandal K, Bhar A & Paul S, Fabrication of PVA-Silver nanoparticle composite film for elimination of microbial contaminant from effluent. *Indian J Biochem Biophys,* 59 (2022) 936.

3 Chen J, Guo Y, Zhang X, Liu J, Gong P, Su Z, Fan L & Li G, Emerging Nanoparticles in Food: Sources, Application, and Safety. *J Agric Food Chem,* 71 (2023) 3564.

4 Setia VY, Dangi K, Biswas L, Singh P & Verma AK, Nano-therapeutic efficacy of green synthesized gold nanoparticles (gAuNPs) and its antibacterial efficacy. *Indian J Biochem Biophys*, 59 (2022) 455.

5 Singh K, Chopra DS, Singh D & Singh N, Green synthesis and characterization of iron oxide nanoparticles using *Coriandrum sativum* L. leaf extract. *Indian J Biochem Biophys,* 59 (2022) 450.

6 Sonali, Rawat A & Yadav M, Nanotechnology in vaccine and immunology. *Indian J Biochem Biophys*, 59 (2022) 1135.

7 Patel HM, Patel BB & Shah CN, Nanosuspension: a novel approach to enhance solubility of poorly water soluble drugs—a review. *Int J Adv Pharm,* 22 (2018) 587.

8 Shid RL, Dhole SN, Kulkarni N & Shid SL, Nanosuspension: a review. *Technology,* 22 (2013) 98.

9 Sutradhar KB, Khatun S, Luna IP. Increasing possibilities of nanosuspension. *J Nanotechnol,* 203 (2013) 1.

10 Samama MM, The mechanism of action of rivaroxaban--an oral, direct Factor X_a inhibitor--compared with other anticoagulants. *Thromb Res,* 127 (2011) 497.

11 Perzborn E, Roehrig S, Straub A, Kubitza D, Mueck W & Laux V, Rivaroxaban: a new oral factor Xa inhibitor. *Arterioscler Thromb Vasc Biol.*, 30 (2010) 376.

12 Perzborn E, Strassburger J, Wilmen A, Pohlmann J, Roehrig S, Schlemmer KH & Straub A, *In vitro* and *in vivo* studies of the novel antithrombotic agent BAY 59-7939—an oral, direct Factor Xa inhibitor. *J Thromb Haemost,* 3 (2005) 514.

13 Rababah TM, Hettiarachchy NS & Horax R, Total phenolics and antioxidant activities of fenugreek, green tea, black tea, grape seed, ginger, rosemary, gotu kola, and ginkgo extracts, vitamin E, and tertbutyl hydroquinone. *J Agric Food Chem,* 52 (2004) 5183.

14 Dixit P, Ghaskadbi S, Mohan H & Devasagayam TPA, Antioxidant properties of germinated fenugreek seed. *Phytother Res*., 19 (2005) 977.

15 Shang M, Cai S, Han J, Li J, Zhao Y, Zheng J, Namba T, Kadota S, Tezuka Y & Fan W, Studies on flavonoids from fenugreek (*Trigonella foenum graecum*). *Zhongguo Zhongyao Zazhi,* 23 (1998) 614.

16 Shlieout G, Arnold K & Muller G, Powder and mechanical properties of microcrystalline cellulose with different degrees of polymerization. *AAPS Pharm Sci Tech,* 3 (2002) E11.

17 Suzuki T & Nakagami H, Effect of crystallinity of microcrystalline cellulose on the compactability and dissolution of tablets. *Eur J Pharm Biopharm,* 47 (1999) 225.

18 Gelman, RA, Characterization of carboxymethyl cellulose—Distribution of substituent groups along the chain. *J Appl Polym Sci,* 27 (1982) 2957.

19 Teather RM & Wood PJ, Use of Congo red polysaccharide interactions in enumeration and characterization of cellulolytic bacteria from the bovine rumen. *Appl Environ Microbiol,* 43 (1982) 777.

20 Chadha R & Bhandari S, Drug–excipient compatibility screening—Role of thermoanalytical and spectroscopic techniques. *J Pharm Biomed Anal,* 87 (2014) 82.

21 Nadendla RR, Satyanarayana J, Shanmukh S, Venkata H, Avinash T, Vishnuvarddhaan A, Katari SK & Kalluri SH, Physico-Chemical Characterization of Rivaroxaban and Compatibility Studies with Its Pharmaceutical Excipients. *Int J Pharm Bio Sci,* 11 (2021) 25.

22 Nadendla RR, Satynarayana J & Burri JK, Rivaroxaban: Compatibilty with Pharmaceutical Excipients using DSC and FTIR Spectrophotometry. *J Pharm Res Int,* 34 (2022) 43.

23 Arya P & Kumar P, Characterization of spray dried diosgen in from fenugreek using binary blend of carrier agents. *Appl Food Res,* 2 (2022) 100054.

24 Liu D, Xu H, Tian B, Yuan K, Pan H, Ma S, Yang X & Pan W, Fabrication of carvedilol nanosuspensions through the anti-solvent precipitation-ultrasonication method for the improvement of dissolution rate and oral bioavailability. *AAPS Pharm Sci Tech,* 13 (2012) 295.

25 Sharannavar B & Sawant S, Formulation and Evaluation of Nanosuspension of Rosuvastatin for Solubility Enhancement by Quality by Design Approach. *IJPSR,* 12 (2021) 5949.

26 Zhang T, Li X, Xu J, Shao J, Ding M & Shi S, Preparation, Characterization, and Evaluation of Breviscapine Nanosuspension and Its Freeze-Dried Powder. *Pharmaceutics,* 14 (2022) 923.

27 Bhargav E, Barghav GC, Reddy YP, Kumar CP, Ramalingam P & Haranath C, A Design of Experiment (DoE) based approach for development and optimization of nanosuspensions of telmisartan, a BCS class II antihypertensive drug. *Future J Pharm Sci,* 6 (2020) 14.

28 Koca M, Sevinç Özakar R, Ozakar E, Sade R, Pirimoğlu B, Özek NŞ & Aysin F, Preparation and Characterization of Nanosuspensions of Triiodoaniline Derivative New Contrast Agent, and Investigation into Its Cytotoxicity and Contrast Properties. *Iran J Pharm Res.,* 21 (2022) e123824.

29 Liu X, Gan H, Hu C, Sun W, Zhu X, Meng Z, Gu R, Wu Z, and Dou G, Silver sulfadiazine nanosuspension-loaded thermosensitive hydrogel as a topical antibacterial agent. *Int J Nanomedicine,* 14 (2019) 289.

30 Ouyang, W, Chen H, Jones ML, Haque T, Martoni C, Afkhami F & Prakash S Novel multi-layer APPPA microcapsules for oral delivery: preparation condition, stability and permeability. *Indian J Biochem Biophys,* 46 (2009) 491.